THE JOURNAL OF BIOLOGICAL CHEMISTRY VOL. 286, NO. 1, pp. 223–233, January 7, 2011

pH-dependent Studies Reveal an Efficient Hydroxylation Mechanism of the Oxygenase Component of *p*-Hydroxyphenylacetate 3-Hydroxylase*[S]

Received for publication, July 12, 2010, and in revised form, September 18, 2010 Published, JBC Papers in Press, October 28, 2010, DOI 10.1074/jbc.M110.163881

Nantidaporn Ruangchan[‡], Chanakan Tongsook[‡1], Jeerus Sucharitakul[§], and Pimchai Chaiyen[‡2]

From the [‡]Department of Biochemistry and Center of Excellence in Protein Structure and Function, Faculty of Science, Mahidol University, Rama 6 Road, Bangkok 10400, Thailand and the [§]Department of Biochemistry, Faculty of Science, Chulalongkorn University, Henri-Dunant Road, Bangkok 10330, Thailand

***p*-Hydroxyphenylacetate (HPA) 3-hydroxylase (HPAH) catalyzes the hydroxylation of HPA at the *ortho*-position to yield 3,4-dihydroxyphenylacetate. The enzyme is a flavin-dependent two-component monooxygenase that consists of a reductase component and an oxygenase component (C_2). C_2 catalyzes the hydroxylation of HPA using oxygen and reduced FMN as co-substrates. To date, the effects of pH on the oxygenation of the two-component monooxygenases have never been reported. Here, we report the reaction kinetics of C_2·$FMNH^-$ with oxygen at various pH values investigated by stopped-flow and rapid quenched-flow techniques. In the absence of HPA, the rate constant for the formation of C4a-hydroperoxy-FMN ($\sim 1.1 \times 10^6\ M^{-1}s^{-1}$) was unaffected at pH 6.2–9.9, which indicated that the pK_a of the enzyme-bound reduced FMN was less than 6.2. The rate constant for the following H_2O_2 elimination step increased with higher pH, which is consistent with a pK_a of >9.4. In the presence of HPA, the rate constants for the formation of C4a-hydroperoxy-FMN ($\sim 4.8 \times 10^4\ M^{-1}s^{-1}$) and the ensuing hydroxylation step (15–17 s^{-1}) were not significantly affected by the pH. In contrast, the following steps of C4a-hydroxy-FMN dehydration to form oxidized FMN occurred through two pathways that were dependent on the pH of the reaction. One pathway, dominant at low pH, allowed the detection of a C4a-hydroxy-FMN intermediate, whereas the pathway dominant at high pH produced oxidized FMN without an apparent accumulation of the intermediate. However, both pathways efficiently catalyzed hydroxylation without generating significant amounts of wasteful H_2O_2 at pH 6.2–9.9. The decreased accumulation of the intermediate at higher pH was due to the greater rates of C4a-hydroxy-FMN decay caused by the abolishment of substrate inhibition in the dehydration step at high pH.**

Flavin-dependent monooxygenases catalyze the incorporation of a single atom of molecular oxygen into organic substrates (1, 2). The enzymes have been classified into six classes according to their catalytic and structural properties. They have also been categorized into two major types according to their protein components: a single-component type, in which reduction of a flavin cofactor and oxygenation of an organic substrate occurs within the same single polypeptide chain; and a two-component type, in which each reaction occurs on separate proteins (1, 2). Single-component monooxygenases have been identified since the 1960s and have been found to be involved in the aerobic metabolism of aromatic and aliphatic compounds in various organisms (2–4). The well known prototype for single-component monooxygenases is *p*-hydroxybenzoate hydroxylase from *Pseudomonas fluorescens* (5, 6). The first enzyme identified as a two-component monooxygenase was bacterial luciferase (7). Nevertheless, most of the two-component monooxygenases have been identified only during the past decade and have increasingly emerged as common enzymes in nature that are involved in many important reactions in various microorganisms (1, 8). Reactions catalyzed by two-component monooxygenases include oxygenation and halogenation of organic compounds such as *p*-hydroxyphenylacetate (9), phenol (10), trichorophenol (11, 12), *p*-nitrophenol (13), styrene (14–16), alkane sulfonate (17, 18), and EDTA (19). Two-component monooxygenases are also involved in oxygenation and halogenation reactions in the biosynthetic pathways of actinorhodin (ActVA) (20), angucyclin (21), enediyne (SgcC) (22), rebeccamycin (RebH) (23), pyrrolnitrin (PrnA) (24), violacein (25), kutzneride (26), and differentiation-inducing factor-1 (27).

All flavin-dependent monooxygenases perform oxygenation through the participation of a reactive intermediate, C4a-hydroperoxy-flavin, which has been well documented and detected by transient kinetics for the reactions of single-component monooxygenases. These monooxygenases include *p*-hydroxybenzoate hydroxylase (PHBH)[3] (5, 6), phenol hydroxylase (28), melilotate hydroxylase (29), antranilate hydroxylase (30), Baeyer-Villiger monooxygenases (31, 32), 2-methyl-3-hydroxypyridine-5-carboxylic oxygenase

* This work was supported by Grants BRG5180002 (to P. C.) and MRG5380240 (to J. S.) from the Thailand Research Fund and a grant from the Faculty of Science, Mahidol University (to P. C.).

[S] The on-line version of this article (available at http://www.jbc.org) contains supplemental "Procedures and Data" and Figs. 1–3.

[1] Supported by the Development and Promotion of Science and Technology Talents Project (Thailand).

[2] To whom correspondence should be addressed. Tel.: 662-2015596; Fax: 662-3547174; E-mail: scpcy@mahidol.ac.th.

[3] The abbreviations used are: PHBH, *p*-hydroxybenzoate hydroxylase; HPA, *p*-hydroxyphenylacetate; HPAH, *p*-hydroxyphenylacetate hydroxylase; DHPA, 3,4-dihydroxyphenylacetate; C_1, the reductase component of HPAH from *A. baumannii*; C_2, the oxygenase component of HPAH from *A. baumannii*; HpaA, the oxygenase component of HPAH from *P. aeruginosa*.

(MHPCO) (33, 34), 2-hydroxybiphenyl 3-monooxygenase (35), and kynurenine 3-monooxygenase (36). For two-component monooxygenases, this intermediate was detected in the reactions of bacterial luciferase (37), *p*-hydroxyphenylacetate hydroxylase (38–40), chorophenol 4-monooxygenase (41), styrene monooxygenase (42), alkane sulfonate monooxygenase (18), and the oxygenases involved in the biosyntheses of rebeccamycin (43) and actinorhodin (44). The mechanistic challenge for these enzymes lies in their ability to control the reactivity of C4a-hydroperoxy-flavin, which is generally manifested through the active site environment. It is known that C4a-hydroperoxy-flavin can act as an electrophile or nucleophile depending on the protonation status of a terminal peroxide group (3, 45, 46). The terminal -OH of C4a-hydroperoxy-flavin is transferred as an electrophile in an electrophilic aromatic substitution reaction, whereas the peroxide group of C4a-peroxy-flavin performs a nucleophilic attack. C4a-hydroperoxy-flavin is commonly found in monooxygenases catalyzing the hydroxylation of aromatic compounds (2, 47–50), whereas C4a-peroxy-flavin is found in Baeyer-Villiger monooxygenases and bacterial luciferase (2, 31, 37, 47). Studies of the PHBH reaction at various pH values have shown that the hydroxylation rate constant is greater at higher pHs because of the deprotonation of the substrate, *p*-hydroxybenzoate, to a phenolate form, which in turn facilitates the electrophilic aromatic substitution reaction (5, 6, 51). To date, none of the two-component monooxygenases have been characterized with respect to the pH dependence of their C4a-(hydro)peroxy-flavin reactivity.

p-Hydroxyphenylacetate hydroxylase (HPAH) from *Acinetobacter baumannii* catalyzes the hydroxylation of *p*-hydroxyphenylacetate (HPA) at the *ortho*-position to yield 3,4-dihydroxyphenylacetate (9). The enzyme serves as an attractive model for investigating how hydroxylation of a phenolic compound can be catalyzed by a two-component monooxygenase. It consists of a smaller reductase component (C_1), which contains FMN as a cofactor, and a larger oxygenase component (C_2), which has no cofactor bound and employs reduced FMN ($FMNH^-$) as a substrate for the hydroxylation of HPA (9, 52). Although it catalyzes a similar *ortho*-hydroxylation of a phenolic compound as single-component hydroxylases, the amino acid sequence (52) and the three-dimensional structure (53) of HPAH compared with single-component monooxygenases are significantly different (1, 5, 52, 53). The active site residues and the binding mode of HPA in C_2 (Fig. 1) are completely different from those of PHBH (5). The active site of C_2 contains a few catalytic residues, which comprise dissociable protons. These residues are in the proper vicinity to participate in the hydroxylation reaction. Therefore, it is interesting to investigate the effects of pH on C_2 hydroxylation.

In addition to HPAH from *A. baumannii*, the structures and catalytic properties of the same enzyme from *Pseudomonas putida* (54), *Escherichia coli* (55), *Pseudomonas aeruginosa* (40), *Sulfolobus tokodaii* (56), and *Thermus thermophilus* HB8 (57) have been reported. Interestingly, HPAHs from all of these species display a certain degree of variation. The size of C_1 is about twice those of other flavin reductases, and it

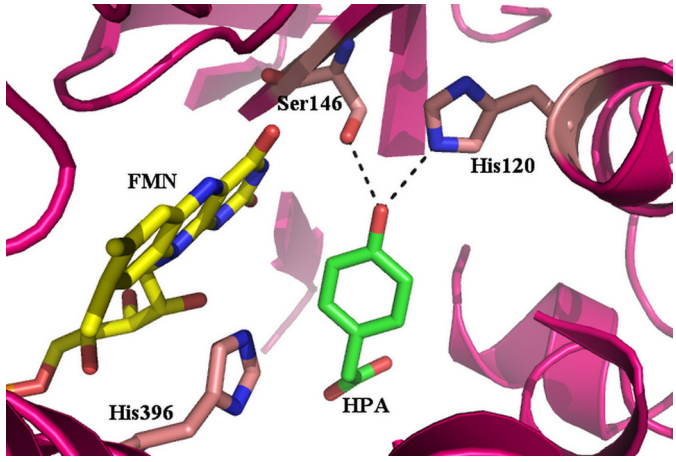

FIGURE 1. **Binding mode of HPA at the active site of C_2.** HPA is shown in *green* and $FMNH^-$ in *yellow*. Residues His-120, Ser-146, and His-396 are labeled.

contains an additional C-terminal regulatory domain (52, 58). The substrate specificity of C_2 is different from other HPAH oxygenases, as C_2 can use $FMNH^-$ and $FADH^-$ equally well (39, 52). The other oxygenases, however, specifically prefer $FADH^-$ (40, 55, 57). A comparison of the structures of C_2 and the oxygenase from *T. thermophilus* HB8 (HpaB) indicates an extra $\beta5$–$\beta6$ loop in *T. thermophilus* HpaB, which facilitates the preferential binding for $FADH^-$ instead of $FMNH^-$ (40, 53, 57). Although the overall structures of C_2 and HpaB from *T. thermophilus* share the same folding of the acyl-CoA dehydrogenase superfamily, the catalytic residues at the active sites of C_2, HpaB, and the oxygenase from *P. aeruginosa* (HpaA) are different (40, 53, 57). These differences indicate that there are different mechanistic details among these enzymes. A previous report has shown that the binding of C_2 to $FMNH^-$ is rapid ($>10^7\ M^{-1}s^{-1}$) (39), enabling efficient transfer of $FMNH^-$ from C_1 to C_2 via diffusion without requiring a protein-protein interaction between the two proteins (59). Recently, it has been shown that the kinetic mechanism of HpaA and the reduced flavin transfer from HpaC (the reductase) to HpaA are different from those of the C_1-C_2 system (40).

With the available knowledge of kinetics and structures of C_2, this enzyme serves as a good model for investigating the effects of pH on the reactivity of C4a-hydroperoxy-flavin. In this report, the reactions of C_2·$FMNH^-$ with oxygen in the presence and absence of HPA at various pH values were investigated using stopped-flow and rapid quenched-flow techniques. These results demonstrate that the hydroxylation by C_2 is unaffected by variations in pH from 6 to 10 in terms of the hydroxylation rate constant and product formation. These results also imply that the optimal interactions among HPA, C4a-hydroperoxy-FMN, and the active site residues are achieved throughout this pH range to allow for effective hydroxylation.

EXPERIMENTAL PROCEDURES

Reagents—The C_1 and C_2 used in this study were cloned, expressed, and purified as described previously (9, 52). All chemicals and reagents used were from commercial sources and of analytical grade. High purity FMN was prepared by

conversion of FAD to FMN using snake venom from *Crotalus adamanteus* (58). Concentrations of the following compounds were determined using known extinction coefficients at pH 7.0: NADH, $\epsilon_{340} = 6.22\ mM^{-1}\ cm^{-1}$; HPA, $\epsilon_{277} = 1.55\ mM^{-1}cm^{-1}$; FMN, $\epsilon_{446} = 12.2\ mM^{-1}cm^{-1}$; 3,4-dihydroxyphenylacetate (DHPA), $\epsilon_{281} = 2.74\ mM^{-1}cm^{-1}$; C_1, $\epsilon_{458} = 12.8\ mM^{-1}cm^{-1}$; C_2, $\epsilon_{280} = 56.7\ mM^{-1}cm^{-1}$. Details for spectroscopic studies and the enzyme assay for C_2 are based on our previous reports (39, 59) and are described in the supplemental material ("Procedures and Data").

Rapid Kinetics Measurements—All reactions were performed with a Hi-Tech Scientific model SF-61DX stopped-flow spectrophotometer (Hi-Tech Scientific, Salisbury, UK) in single mixing mode at 4 °C. Details for the rapid kinetics measurements are described in the supplemental material. The methods used for studying the reactions of C_2 with oxygen were similar to those used previously (39), except dithiothreitol (DTT) was removed from the enzyme solution prior to the experiments. The buffers used for maintaining various pH values were 100 mM sodium phosphate buffer, pH 6.0–7.5, 100 mM Tris-HCl buffer, pH 8.0–8.5, and 100 mM glycine adjusted with NaOH, pH 9.0–10.0. Stopped-flow experiments were monitored for absorbance changes at 380 and 446 nm. For product analysis, about four shots from the stopped-flow mixing were collected at each pH after the reaction was complete. HCl was added to the collected sample to a final concentration of 0.08 M, and the solution was passed through an ultrafiltration unit (Microcon) with a molecular weight cut-off of 10,000 to collect the filtrate. The quantity of DHPA in each sample was determined using HPLC analysis as described previously (9, 52).

Rapid Acid-quenched Experiments—C_2 reactions at various pH values and at 4 °C were acid-quenched using a Hi-Tech Scientific model RQF-63 Dimention™ D1 rapid quenched-flow system in an anaerobic glovebox (Belle Technology). This rapid quenched-flow system employs three syringes. An anaerobic solution of C_2, FMN, and HPA in 10 mM sodium phosphate buffer, pH 7.0, was reduced with a solution of sodium dithionite in the anaerobic glovebox. A solution of the reduced enzyme-substrate complex (C_2·$FMNH^-$·HPA) from one syringe was mixed with the oxygenated buffers and HPA at various pHs from a second syringe. The reaction mixtures were allowed to age for various time periods and were then quenched by mixing with 0.15 M HCl from a third syringe. After mixing and prior to quenching, the reaction contained C_2 (100 μM), $FMNH^-$ (50 μM), HPA (2 mM), and oxygen (0.13 mM). The final pH of the quenched reaction mixture was 1.4. The mixtures contained soluble but denatured C_2, which was removed by ultrafiltration using a Microcon unit with a molecular weight cut-off of 10,000 (Amicon YM-10). The Microcon was centrifuged at 10,000 rpm for 30 min at 4 °C, and ~100 μl of filtrate was obtained. The amount of DHPA in each quenched reaction was determined using the HPLC method (9).

Determination of Hydrogen Peroxide Formed—Measurements of oxygen consumption and H_2O_2 formation at various pHs were carried out in closed reaction vessels (3 ml total volume) fitted with a Clark-type oxygen electrode and a magnetic stirrer (Yellow Springs Instruments, model 53 oxygen monitor) (9). The assay reaction contained 150 μM NADH, 2 mM HPA, 10 μM FMN, 10 nM C_1, and 3.35 μM C_2 in buffers, pH 6–10. The buffers used were 100 mM sodium phosphate for pH 6.0–7.0, 100 mM Tris-HCl for pH 8.0, and 100 mM glycine-NaOH for pH 9.0–10.0. To begin oxygen consumption, the reaction was initiated by adding NADH (final concentration of 150 μM (100 μl)). Reaction completion was indicated by a steady level of O_2 consumption, and catalase (20 units, 100 μl) was then added to the reaction mixture to convert H_2O_2 to O_2. The amounts of H_2O_2 are equivalent to two times each mole of oxygen generated after adding catalase. A buffer solution (100 μl) was added to the vessel at the end of the reaction to calculate the oxygen increment due to sample adding. In addition, the determination of H_2O_2 from single turnovers was carried out using a peroxidase-coupled assay as described in the supplemental "Procedures and Data." The limit of detection for the peroxidase assay was 1% H_2O_2.

Data Analysis—Stopped-flow traces were analyzed by Program A (written at the University of Michigan by Rong-yen Chu, Joel Dinverno, and D. P. Ballou) or KinetAsyst 3 software (Hi-Tech Scientific). Data from rapid-quench experiments were analyzed using exponential fits based on the Marquardt-Levenberg nonlinear fitting algorithms, which were included in the KaleidaGhaph software (Synergy Software).

RESULTS

Reaction of C_2·$FMNH^-$ with Oxygen—Previous results from the reaction of C_2·$FMNH^-$ with oxygen have shown that the observed rate constants of C(4a)-hydroperoxy-FMN formation are linearly dependent on oxygen concentrations, with a bimolecular rate constant of $1.1 \times 10^6\ M^{-1}s^{-1}$. The intermediate decays to form hydrogen peroxide (H_2O_2) with a first-order rate constant of $0.037\ s^{-1}$ (39). This reaction was carried out in the presence of 0.5 mM DTT. In this study, the reaction of C_2·$FMNH^-$ with oxygen in the presence and absence of HPA were reinvestigated in the absence of DTT.

The reduced enzyme (C_2·$FMNH^-$) in 50 mM sodium phosphate buffer, pH 7.0, was mixed with buffers containing various oxygen concentrations. The conditions used for these experiments were similar to those in the previous report (39), except the enzyme concentration was increased from 25 to 35 μM. After mixing, the reaction contained C_2 (35 μM), $FMNH^-$ (16 μM), and oxygen (0.13, 0.31, 0.61, and 1.03 mM). The reactions were monitored for absorbance changes at 380 and 446 nm, and the reaction kinetics were found to be biphasic (supplemental Fig. 1). The first phase was a bimolecular reaction, which represents the formation of C(4a)-hydroperoxy-FMN as its absorbance at 380 nm, increased with no change in absorbance at 446 nm (supplemental Fig. 1 and 39). A plot of the observed rate constants (k_{obs}) of this phase *versus* the oxygen concentrations was linear and showed the same value as the published value of $1.1 \times 10^6\ M^{-1}s^{-1}$ at 4 °C and pH 7.0 (39). The second kinetic phase resulted in a decrease of absorbance at 380 nm and a large increase of absorbance at 446 nm, indicating that this phase corresponded to H_2O_2 elimination from the C(4a)-hydroperoxy-FMN. This phase was concomitant with the formation of the oxidized enzyme (supplemental Fig. 1).

Analysis of this phase yielded a rate constant of 0.003 s^{-1} at all oxygen concentrations, which was about 12-fold less than the value obtained from the reaction in the presence of 0.5 mM DTT (39). It is currently unknown how DTT enhances this H_2O_2 elimination process.

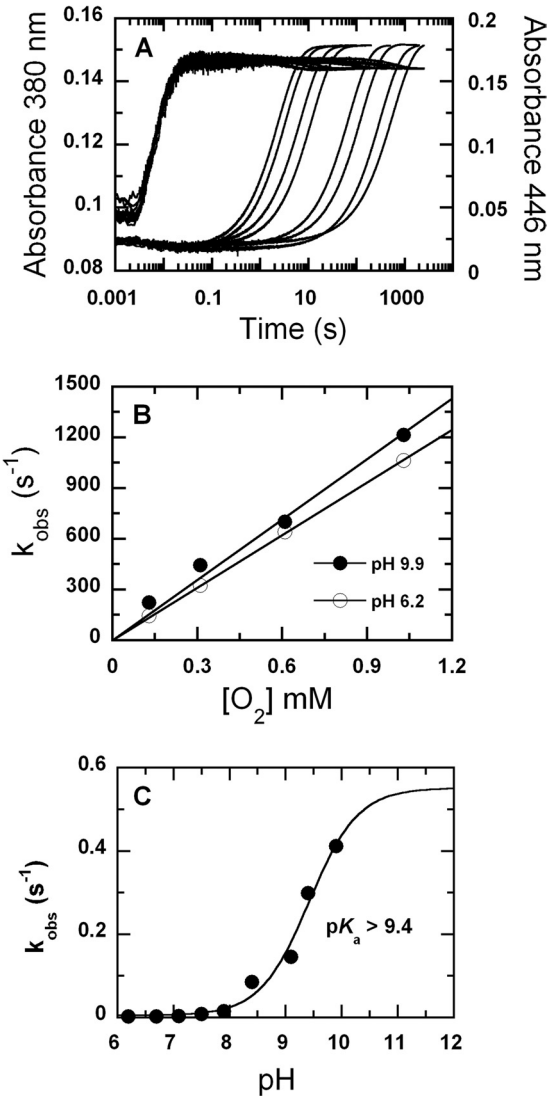

FIGURE 2. **Reactions of C_2·FMNH$^-$ with oxygen at various pHs.** *A*, a solution of the reduced enzyme (C_2·FMNH$^-$) was mixed with buffers containing oxygen at various pHs using the stopped-flow spectrophotometer. The reactions were monitored for absorbance changes at 380 and 446 nm. After mixing, the reactions contained C_2 (35 μM), FMNH$^-$ (16 μM), and oxygen (1.03 mM). The final pH values were 6.2, 6.7, 7.1, 7.5, 7.9, 8.4, 9.1, 9.4, and 9.9. The *traces* at 446 nm are shown from *right* to *left* according to low to high pH values, whereas those of 380 nm are according to the *upper* to *lower traces*. *Traces* at pH 6.2 and 6.7 are identical and superimposed on each other. *B*, plots of k_{obs} of C4a-hydroperoxy-FMN formation *versus* the oxygen concentrations at pH 6.2 (*empty circles*) and 9.9 (*filled circles*). *C*, a plot of rate constants for the H_2O_2 elimination step *versus* pH. The values are 0.0017, 0.0018, 0.0033, 0.0081, 0.015, 0.085, 0.145, 0.30, and 0.41 s^{-1} at pH 6.2, 6.7, 7.1, 7.5, 7.9, 8.4, 9.1, 9.4, and 9.9, respectively.

Reaction of C_2·FMNH$^-$ with Oxygen at Various pHs—A solution of the reduced enzyme (C_2·FMNH$^-$) in 10 mM sodium phosphate buffer, pH 7.0, was mixed with buffers of various oxygen concentrations at pH 6–10. The buffers used were 100 mM sodium phosphate for pH 6.0–7.5, 100 mM Tris-HCl for pH 8.0–8.5, and 100 mM glycine-NaOH for pH 9.0–10.0. After mixing, the reaction contained C_2 (35 μM), FMNH$^-$ (16 μM), and oxygen (0.13, 0.31, 0.61, and 1.03 mM) at final pH values of 6.2, 6.7, 7.1, 7.5, 7.9, 8.4, 9.1, 9.4, and 9.9. The results displayed are those with 1.03 mM oxygen. The data showed that at all pH values, the reaction consisted of two phases (Fig. 2*A*). The first phase was the formation of C(4a)-hydroperoxy-FMN, as shown by the absorbance increase at 380 nm without any change at 446 nm. The second phase was the elimination of H_2O_2 from C(4a)-hydroperoxy-FMN to generate oxidized flavin, as indicated by a large absorbance increase at 446 nm (Fig. 2*A*). The rate constants for the formation of C(4a)-hydroperoxy-FMN were independent of pH and were almost constant at 1.1×10^6 $M^{-1}s^{-1}$ (Figs. 2*B* and 3). This implies that at all pH values, the reduced flavin is likely to be in the anionic form (deprotonated at the flavin N1) because this form of reduced flavin reacts rapidly with oxygen (45, 46). It also suggests that the pK_a of reduced FMN bound to C_2 is lower than 6.0 because the rate constant of this phase did not significantly change with pH variation (Fig. 2*B*). In contrast, the rate constant of the second phase, the elimination of H_2O_2, increased with higher pH values and was associated with a pK_a of >9.4 (Fig. 2*C*). Although a curve associated with a pK_a of 9.4 can fit the plot in Fig. 2*C*, it is likely that the real pK_a value is higher than 9.4 because the curve has not reached saturation. The highest pH investigated was limited to pH 10.0 because C_2 becomes denatured above this pH. This pK_a may be due to the deprotonation at flavin N5 of C(4a)-hydroperoxy-FMN to eliminate H_2O_2 as a leaving group, or it may be due to the residue acting as a general base in H_2O_2 elimination. A summary for the C_2 reaction in the absence of HPA is described in Fig. 3.

Reaction of C_2·FMNH$^-$·HPA with Oxygen at Various pHs—A solution of the reduced enzyme plus HPA (C_2·FMNH$^-$·HPA) in 10 mM sodium phosphate buffer, pH 7.0, was mixed with buffers equilibrated with various oxygen concentrations at pH 6–10 in the stopped-flow spectrophotometer. The buffers used were 100 mM sodium phosphate for pH 6.0–7.5, 100 mM Tris-HCl for pH 8.0–8.5, and 100 mM glycine-NaOH for pH 9.0–10.0. After mixing, the reactions contained C_2 (35 μM), FMNH$^-$ (16 μM), HPA (2 mM) and oxygen (0.13, 0.31, 0.61, and 1.03 mM), and the final pHs were 6.2, 6.7, 7.1, 7.5, 7.9, 8.4,

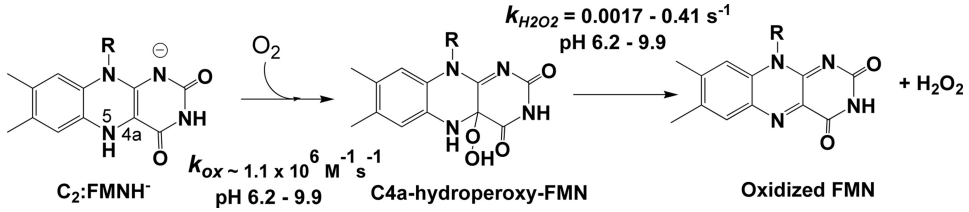

FIGURE 3. **Reaction of C_2 in the absence of HPA at various pHs.** Positions N5 and C4a of the isoalloxazine ring are labeled at the C_2·FMNH$^-$ structure.

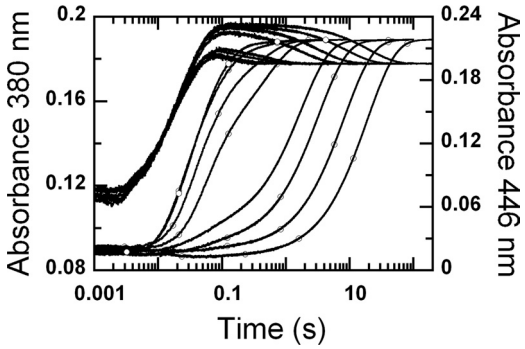

FIGURE 4. **Reactions of the C_2·FMNH$^-$·HPA complex with oxygen at various pH.** A solution of the reduced enzyme (C_2·FMNH$^-$·HPA) was mixed with buffers containing oxygen plus HPA at various pH in the stopped-flow spectrophotometer. The reactions were monitored for absorbance changes at 380 (*lines*) and 446 nm (*lines* with *empty circles*). After mixing, the reaction contained C_2 (35 μM), FMNH$^-$ (16 μM), HPA (2 mM), and oxygen (1.03 mM). Absorbance *traces* at 446 nm are shown from *right* to *left* according to pH 6.2, 6.7, 7.1, 7.5, 7.9, 8.4, 9.3, and 9.9, and those at 380 nm are shown from *upper* to *lower traces* as the pH increases.

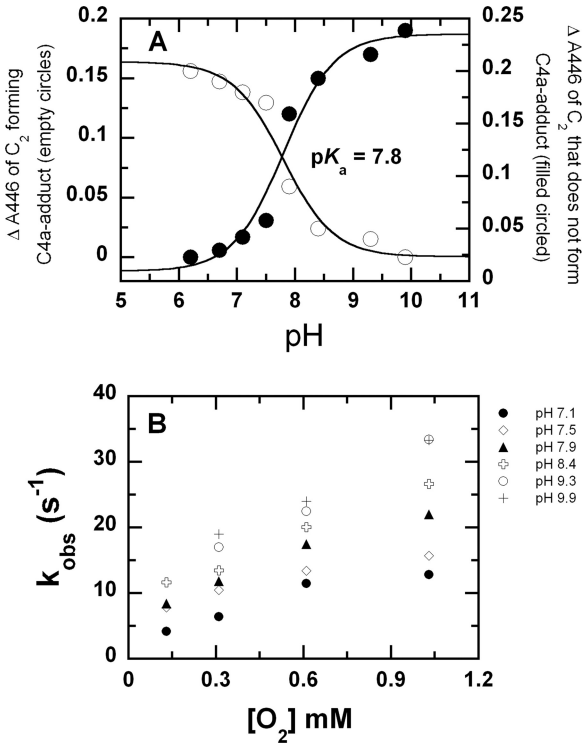

FIGURE 5. **Analysis of data from the reactions of the C_2·FMNH$^-$·HPA complex with oxygen at various pHs.** *A*, shows a plot of the amplitude changes at A_{446} from the pathway that accumulates the C4a-adduct intermediate (*empty circles*) and from the pathway that does not accumulate the C4a-adduct intermediate (*filled circles*) *versus* pH. Data are from Fig. 4. A theoretical curve for a single ionization process with a pK_a value of 7.8 can be fitted to both plots. *B*, shows a plot of k_{obs} from the second phase of A_{446} (from the pathway without C4a-adduct accumulation) at various pH values *versus* the oxygen concentrations.

9.3, and 9.9. Kinetic traces displayed in Fig. 4 represent those from the reactions with 1.03 mM oxygen. The reactions were followed by monitoring absorbance changes at 380 nm and 446 nm.

The results (Fig. 4) show that kinetic traces monitored at 380 nm consisted of three phases. The first phase was a small increase in absorbance (up to 0.007 s), which was dependent on oxygen concentration, with a bimolecular rate constant of 1.1×10^6 M^{-1}s^{-1}, and independent of pH. This phase was interpreted as the reaction between a small fraction of C_2 without HPA bound (C_2·FMNH$^-$) and oxygen to form C(4a)-hydroperoxy-flavin, as in the reaction in Fig. 2. The second phase showed an increase in absorbance at 380 nm (0.007–0.09 s), which was larger than the first phase (Fig. 4). The observed rate constants of this phase were dependent on oxygen concentration and independent of pH (supplemental Fig. 2). This phase was interpreted as the reaction of C_2·FMNH$^-$·HPA with oxygen to form C(4a)-hydroperoxy-FMN·HPA with a bimolecular rate constant of 4.8×10^4 M^{-1}s^{-1} (39). Therefore, the rate constants of the first and second phases were not affected by pH, implying that at all pH levels, reduced FMN bound in the C_2·FMNH$^-$ or C_2·FMNH$^-$·HPA complexes was in the anionic form and that the pK_a of $FMNH_2$ should be less than 6.0. The third phase (0.09 s until the completion of the reaction) had an absorbance decrease at 380 nm (~0.017 AU at pH 6.2–7.5 and less than 0.007 AU at pH 7.9 and higher (Fig. 4)). Therefore, this phase represents the decay of a flavin C4a-adduct intermediate (C4a-hydroperoxy-FMN or C4a-hydroxy-FAD) to the oxidized enzyme. On the basis of these data alone, a species of the flavin C4a-adduct cannot be assigned, as our previous data indicate that the spectra of C4a-hydroperoxy-FMN and C4a-hydroxy-FMN bound to C_2 are very similar and that both have an absorption peak at ~380 nm (39). The observed rate constant of this phase was dependent on pH (supplemental Fig. 3).

Kinetic traces monitored at 446 nm showed three phases. The first phase represents a small lag in absorbance decrease, which was synchronized with the change of the second phase monitored at 380 nm. The observed rate constants of this phase were dependent on oxygen concentration and independent of pH in the same manner as the second phase monitored at A_{380}. Therefore, this phase was the reaction of C_2·FMNH$^-$·HPA with oxygen to form C4a-hydroperoxy-FMN·HPA. The second phase of the traces monitored at 446 nm showed an absorbance increase, and its amplitude and rate constant were dependent on pH (Fig. 5). The amplitude of this phase at $A_{446\ nm}$ increased with increasing pH, *i.e.* from ~ 0.017 AU (0.015–0.2 s) at pH 7.1 to ~0.19 AU (0.007–0.15 s) at pH 9.9. A plot of the amplitude change *versus* pH was consistent with a curve associated with a pK_a of 7.8 (Fig. 5*A*). Rate constants of this phase increased according to the oxygen concentration and pH (Fig. 5*B*). At an oxygen concentration of 1.03 mM, the observed rate constant of this phase increased from 12 s^{-1} at pH 7.1 to 33 s^{-1} at pH 9.9 (Fig. 5*B*). Therefore, this phase represents the formation of oxidized FMN without an apparent detection of the flavin C4a-adduct intermediate. The third kinetic phase monitored by an absorbance change at 446 showed an absorbance increase, which was dependent on pH but not on oxygen concentration. The observed rate constants of this phase were the same as those of the last phase monitored at 380 nm. Therefore, this phase represents the formation of oxidized FMN from the flavin C4a adduct intermediate. The amplitude of this phase decreased with higher pH in a reciprocal fashion to the amplitude change of the second phase at 446 nm (Fig. 5*A*). Plots of the amplitude changes *versus* pH for both the second

and third phases were consistent with an ionizable group with a pK_a of 7.8 (Fig. 5*A*). Therefore, the second and third phases observed at 446 nm represent two pathways in which the enzyme returns to the oxidized species. The partition between the two pathways was controlled by the pH of the reaction, and the pK_a associated with this partition was ~7.8. One pathway that was more prominent at a lower pH was formation of the oxidized flavin via a detectable C4a-adduct intermediate, as shown by the third phase of A_{380} and A_{446}. Upon an increase in pH, more of the enzyme returned to the oxidized FMN via the pathway that did not allow detection of the C4a-adduct intermediate (the second phase of the traces at 446 nm).

Measuring Rate Constants for Hydroxylation at Various pHs Using Rapid-quench Techniques—Reactions of the C_2·FMNH$^-$·HPA complex with oxygen at various pHs resulted in the formation of flavin C4a-adduct intermediates (Figs. 4 and 5). In principle, to generate the product, the reaction should initially form C4a-hydroperoxy-FMN and be followed by the hydroxylation of HPA and the formation of C(4a)-hydroxy-FMN. However, on the basis of the flavin absorption data alone, the hydroxylation rate constant in the C_2 reaction cannot be measured accurately because the absorption properties of C4a-hydroperoxy-FMN and C4a-hydroxy-FMN are very similar (39). The hydroxylation rate constant at pH 7.0 was approximated to be ~17–22 s^{-1} based on the stopped-flow data (39). In this study, to investigate the effects of pH on the hydroxylation step, rapid acid-quench techniques were used to measure the rate constants of product formation. The rapid-quench apparatus employed a three-syringe system. The reduced enzyme-substrate complex (C_2·FMNH$^-$·HPA) in 10 mM sodium phosphate buffer, pH 7.0, at 4 °C from one syringe was mixed with air-saturated buffers containing HPA at various pHs from a second syringe. The reaction mixture was allowed to age for a specified time period and was then quenched by mixing with 0.15 M HCl from a third syringe. After mixing but before quenching, the reaction contained C_2 (100 μM), FMNH$^-$ (50 μM), HPA (2 mM), and oxygen (0.13 mM) at pH 6.2, 7.1, 7.9, and 9.3. The final pH of the quenched reaction was 1.4. The amount of DHPA formed at each quenching point was determined using the HPLC method ("Experimental Procedures"). Plots of DHPA formed *versus* the age times at pH 6.2 and 9.3 yielded single exponential curves, as shown in Fig. 6. Rate constants of the hydroxylation step at various pH values are shown in Table 1. The results indicated that the hydroxylation rate constants were in the range of 15 to 17 s^{-1} at all pHs investigated. These data also imply that the reactions in Fig. 4 initially formed C4a-hydroperoxy-FMN, which was followed by hydroxylation to yield C4a-hydroxy-FMN and DHPA (Fig. 7, *steps a* and *b*) before forming the oxidized enzyme.

Hydroxylation Ratios of C_2 Reactions at Various pHs—The reaction of C_2·FMNH$^-$·HPA with oxygen monitored by stopped-flow spectrophotometry (Fig. 4) indicated that the enzyme returned to oxidized FMN via two pathways. The pathway dominant at lower pH (pH 6.2–8) allowed for the detection of a flavin C4a-adduct. Based on the rapid-quench

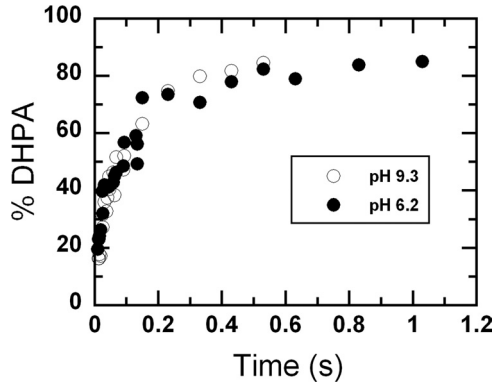

FIGURE 6. **Rapid acid-quench of the reactions of C_2·FMNH$^-$·HPA with oxygen at pH 6.2 (*filled circles*) and 9.3 (*empty circles*).** Reactions of C_2·FMNH$^-$·HPA with oxygen were quenched with 0.15 M HCl at various times using the rapid-quench apparatus. After mixing and prior to quenching, the reactions contained C_2 (100 μM), FMNH$^-$ (50 μM), HPA (2 mM), and oxygen (0.13 mM) at pH 6.2 (*filled circles*) or 9.3 (*empty circles*). The final pH of the quenched reaction mixture was 1.4. A plot of DHPA formed *versus* quenched times yielded a single exponential curve with a rate constant of 17 ± 2 s^{-1} at pH 6.2 and 15 ± 1 at pH 9.3. At the age time of ~10 s, the percentages of DHPA formed were around 90%.

TABLE 1
Hydroxylation ratios of C_2 reaction

pH	Rate constant of hydroxylation	Percentage of DHPA formed per FMNH$^-$ used[a]
	s^{-1}	
6.2	17 ± 2	90 ± 5
6.6		91 ± 4
7.1	16 ± 2	89 ± 5
7.5		89 ± 6
7.9	17 ± 2	92 ± 4
8.4		90 ± 3
9.3	15 ± 1	92 ± 2
9.8		89 ± 4

[a] Measurements of H_2O_2 were carried out as described under "Experimental Procedures" to determine whether the ~10% product loss was due to H_2O_2 formation. H_2O_2 in a range of 0.5 to 2% was detected independently of pH. Therefore, C_2 catalyzed an efficient hydroxylation reaction without significant formation of H_2O_2 from the uncoupling pathway, and ~10% of the product loss was due to sample loss during the preparation process prior to the HPLC measurement.

data (Fig. 6, Table 1, and the previous section), the intermediate observed at ~0.2 s in Fig. 4 can be assigned as C4a-hydroxy-FMN. At higher pH values (pH 8.4–10.0), the majority of the reaction did not result in a detectable intermediate (Figs. 4 and 5). The immediate question that arose was whether both pathways catalyzed a productive hydroxylation to form DHPA. Therefore, the amount of DHPA formed from a single turnover reaction at each pH was measured. The results in Table 1 indicated that at all pH values, the reaction yielded similar hydroxylation ratios of ~90% (ratios of product per reduced flavin), in agreement with the hydroxylation rate constants at all pH values (Table 1 and Fig. 6). Measurements of H_2O_2 were also carried out to clarify whether ~10% of the product loss was due to H_2O_2 formation ("Experimental Procedures"). The results indicated that only 0.5–2% of the H_2O_2 was detected at all pHs (data not shown). Determination of H_2O_2 from single turnovers was also carried out using a peroxidase-coupled assay that measured H_2O_2 with a detection limit of 1% (supplemental "Procedures and Data"). The measurements could not detect any H_2O_2 formation, which confirmed that no significant amount of H_2O_2 was generated at pH 6–10. Therefore, C_2 catalyzed an efficient hydroxyla-

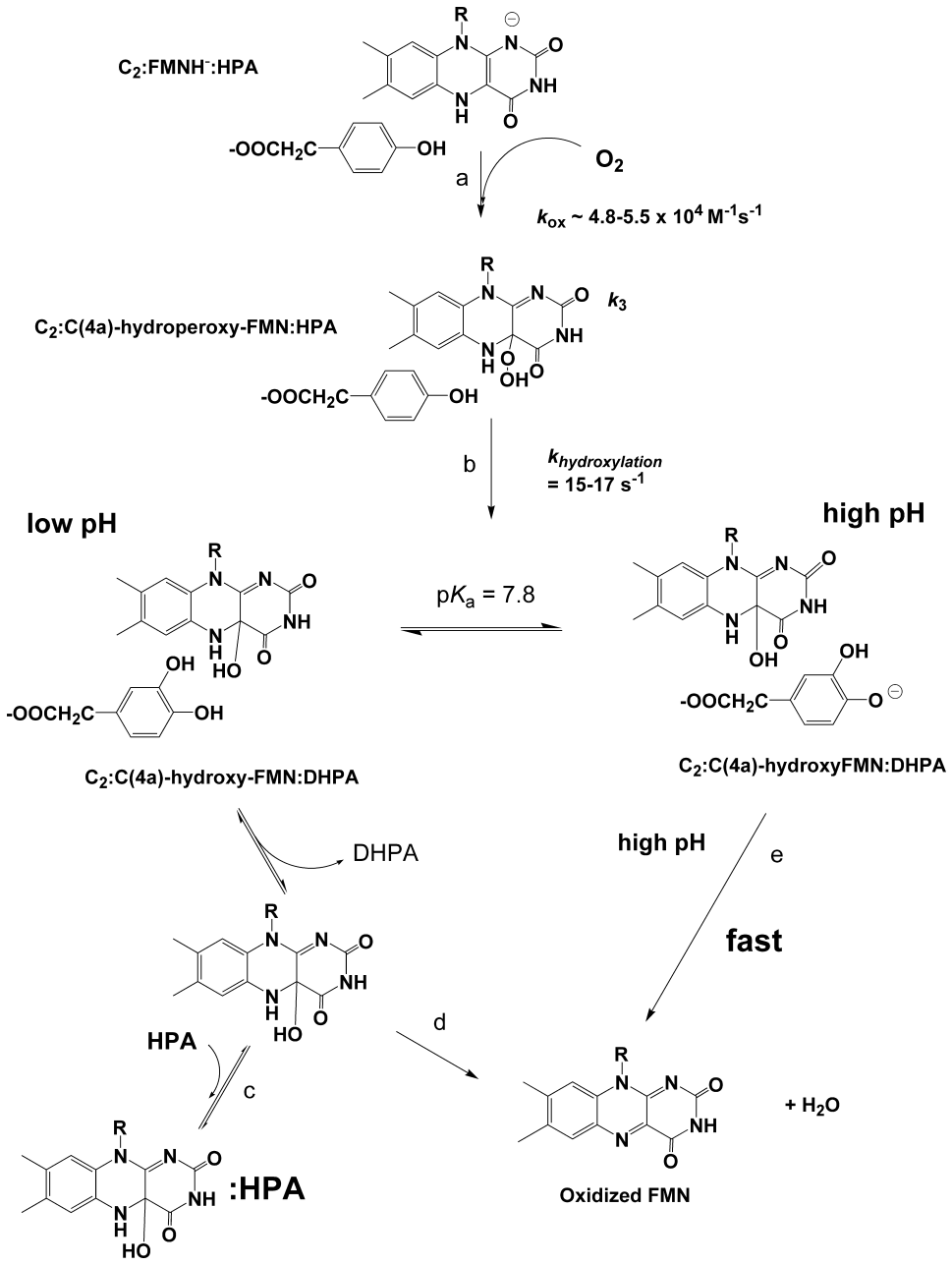

FIGURE 7. **The reaction of C_2 at low and high pHs.** At low pHs, after hydroxylation (*step b*), DHPA dissociates and excess HPA binds to the C_2 active site (*step c*), trapping and allowing the detection of C4a-hydroxy-FMN before dehydration (*step d*). At high pHs, after hydroxylation (*step b*), the dehydration (*step e*) to generate the oxidized FMN is rapid, preventing accumulation and detection of C_2·C4a-hydroxy-FMN.

tion reaction because the formation of H_2O_2 from the uncoupled pathway was not significant. The product loss of ~10%, as indicated in Table 1, was most likely due to loss during sample handing prior to the HPLC detection.

These results indicate that at all pH values, C_2 can efficiently catalyze HPA hydroxylation. The reactions in Fig. 4 occur via formation of C4a-hydroperoxy-FMN, followed by hydroxylation to yield C4a-hydroxy-FMN and DHPA (Fig. 7, *steps a* and *b*). At lower pHs, the pathway that allows detection of C4a-hydroxy-FMN prior to the oxidation step is more prominent (Fig. 7, *left pathway*). At higher pHs (Fig. 7, *right pathway*), more of the enzyme returns to the oxidized FMN via the pathway that does not allow detection of the C4a-hydroxy-FMN, possibly because of the rapid dehydration of C4a-hydroxy-FMN to form oxidized FMN.

We propose that at low pH, excess HPA binds to C4a-hydroxy-FMN (Fig. 7, *step c*) and inhibits the dehydration of C4a-hydroxy-FMN to form oxidized FMN (Fig. 7, *step d*) and that this allows the detection of C4a-hydroxy-FMN. At high pH, flavin oxidation (Fig. 7, *step e*) occurs rapidly due to the abolishment of HPA inhibition as in the low pH condition. Therefore, at high pH, the reaction does not allow for the detection of the C4a-hydroxy-FMN intermediate. Kinetic mechanisms of C_2 at different pH values are summarized in Fig. 7.

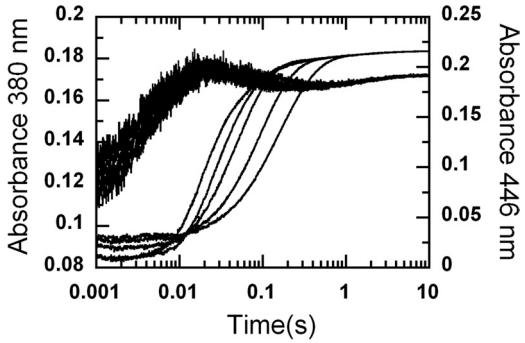

FIGURE 8. **Reactions of C_2·FMNH$^-$ with oxygen and HPA at various concentrations at pH 9.0.** A solution of the reduced enzyme (C_2·FMNH$^-$) was mixed with buffers containing oxygen and various concentrations of HPA in the stopped-flow spectrophotometer. The reactions were monitored for absorbance changes at 380 and 446 nm. After mixing, the reaction contained C_2 (35 μM), FMNH$^-$ (16 μM), oxygen (0.13 mM), and various concentrations of HPA. Absorbance *traces* at 446 nm are shown from *right* to *left* according to the HPA concentrations of 80, 160, 400, 800, and 2000 μM, and the *traces* at 380 nm are shown from *left* to *right* as the HPA concentration increases.

Inhibition of the Dehydration Step by HPA at pH 9.0—It is commonly known that aromatic substrates at high concentrations exhibit inhibitory effects on the dehydration of C4a-hydroxy-FMN (5, 28, 33). For the C_2 reaction at pH 7.0, excess HPA binds to the C4a-hydroxy-FMN intermediate with the K_d value of 41 μM (39). The data in the previous section imply that the decrease of C4a-hydroxy-FMN detected at higher pHs was due to the greater rates of intermediate decay. This fast decay process might be because of the abolishment of the substrate inhibitory effect during the dehydration step (Fig. 7, *steps c* and *d*).

When C_2 reactions were carried out at pH 9.0 in the presence of various concentrations of HPA, the dehydration of C4a-hydroxy-FMN to yield oxidized FMN (Fig. 7, *step e*) was not inhibited at higher concentrations of HPA (Fig. 8), unlike the reaction at pH 7.0 (39). In addition, the rates for flavin oxidation (a large increase in A_{446}) were faster at higher HPA concentrations (Fig. 8) as opposed to the data at pH 7.0 (39). This result supports the kinetic model described in Fig. 7 showing that at high pHs, excess HPA cannot inhibit the dehydration of the C4a-hydroxy-FMN intermediate because of the abolishment of excess HPA binding. This may be caused by a very fast dehydration process of C4a-hydroxy-flavin at pH 9.0, *i.e.* the dehydration of C4a-hydroxy-FMN may occur before the excess HPA can bind (see more under "Discussion"). The slower rates of flavin oxidation (absorbance increase at A_{446} (Fig. 8)) at lower HPA concentrations was due to the existence of the HPA-free enzyme. At HPA concentrations lower than 2.0 mM, some fraction of the enzyme was in the HPA-free form similar to the reaction in Fig. 2. The HPA-free form results in the formation of C4a-hydroperoxy-FMN, which eliminates H_2O_2 to generate oxidized FMN at a slower rate (Figs. 2 and 3).

DISCUSSION

Our report elucidates the kinetics of C_2·FMNH$^-$ with oxygen at various pH values and demonstrates that the hydroxylation by C_2 is highly efficient. The kinetics of C_2 reactions in the absence and presence of HPA, at various pH values, provided insight into nature and catalytic properties of the C4a-hydroperoxy-flavin intermediate of this enzyme. In the absence of HPA, C_2 formed C4a-hydroperoxy-FMN, which eliminated H_2O_2 to generate oxidized FMN (Fig. 3). The intermediate was more stable at lower pHs because a rate constant for H_2O_2 elimination increased when the pH was increased. The plot of the observed rate constants *versus* pH (Fig. 2*C*) was consistent with a pK_a of >9.4, indicating that the H_2O_2 elimination process occurred faster at higher pHs. This pK_a may be due to the deprotonation of the flavin N5 proton to initiate H_2O_2 elimination or to the residue acting as a general base to abstract the flavin N5 proton. According to NMR measurements, the pK_a of the N5 proton of free reduced FMN was estimated at >20 (60). The pK_a of the N5-H of C4a-hydroperoxy-flavin is expected to be at least 3–4 units below the pK_a value of the N5-H of reduced flavin because the C4a-hydroperoxy flavin is neutral, not anionic as in the reduced flavin (61). Merényi and Lind (61) estimated a pK_a value for the N5 proton of C4a-hydroperoxy-flavin to be less than 17. When a pK_a associated with the H_2O_2 elimination from C4a-hydroperoxy-flavin is considered, other factors must be taken into account. It can be envisaged that the change of flavin N5 hybridization upon elimination of H_2O_2 can favor the deprotonation of flavin N5-H. Rate constants of H_2O_2 elimination from 5-alkylated-C4a-hydroperoxy-flavin synthesized from pulse radiolysis were measured at various pHs and found to be consistent with a pK_a of >10 (61). Here, we propose that the pK_a of >9.4 observed with H_2O_2 elimination from C4a-hydroperoxy-flavin (Figs. 2 and 3) is largely associated with a pK_a of the flavin N5-H.

It should be noted that, in theory, the terminal hydroperoxide group of C4a-hydroperoxy-FMN may have a pK_a of ~9.4. The pK_a of H_2O_2 is ~11.8 (62), whereas the pK_a of a flavin C4a-hydroperoxide can be significantly different from this value, depending on the enzyme active site environment. On the basis of the results obtained from studying flavin model compounds, a pK_a of free flavin C4a-hydroperoxide was estimated to be ~9.2 (63). However, the deprotonation of a terminal hydroperoxide group disfavors H_2O_2 elimination, because hydroperoxide is a better leaving group. Therefore, the higher rate constant of the H_2O_2 elimination step observed at higher pHs (Fig. 2) should not be due to deprotonation of the hydroperoxide group. In addition, results from the product analysis (Table 1) also indicate that the terminal hydroperoxide group of C4a-hydroperoxy-FMN remains protonated, as the hydroxylation is efficient throughout this pH range (see more below). Therefore, it is unlikely that the pK_a of >9.4 in Fig. 2 belongs to the deprotonation of flavin C4a-hydroperoxide.

C4a-hydroperoxy-flavin, found in the C_2 reaction in the absence of HPA, was relatively stable at neutral pH, because the rate constant for this intermediate decay was 0.003 s^{-1}, which is equivalent to a half-life of ~231 s at pH 7.0. The slow elimination of H_2O_2 from the C4a-hydroperoxy-FMN intermediate in C_2 provides another means of preventing wasteful H_2O_2 generation in the absence of HPA in addition to the regulation by HPA-stimulated activity of the C_1 component

(58, 59). For the reaction of HpaA from *P. aeruginos*a in the absence of HPA, C4a-hydroperoxy-flavin forms with a bimolecular rate constant of 3×10^5 $M^{-1}s^{-1}$ and decays with a rate constant of 0.005 s^{-1}. It is thought that at low concentrations of HPA, the majority of *in vivo* HpaA exists in the form of C4a-hydroperoxy-FAD (40). The same scenario is also applicable for the C_1-C_2 reaction, as the H_2O_2 elimination step (rate constant of 0.003 s^{-1}) is the slowest step in the overall reaction of C_1 and C_2 in the absence of HPA (39, 58, 59). C4a-hydroperoxy-flavin is also generally stable in the other two-component monooxygenases, such as in the reaction of bacterial luciferase where the rate constant for the H_2O_2 elimination is 0.002 s^{-1} at pH 8.0 (37) and in actinorhodin where it decays with a half-life of 1400 s at pH 7.4 (44). The intermediate is also stable in the reaction of cyclohexanone monooxygenase, as the flavin oxidation completed within 10,000 s at pH 7.2 and 1,900 s at pH 9.0 (31). All of the above rate constants were measured at 4 °C. On the contrary, most single-component aromatic hydroxylases do not stabilize C4a-hydroperoxy-flavin in the absence of aromatic substrates because the reduced enzymes react with oxygen to form the oxidized enzymes in a second-order fashion without any detectable intermediates (5, 47, 50). The differences in the degree of C4a-hydroperoxy-flavin stability among these enzymes must be due to the differences in their active site environments.

Rapid-quench techniques allowed us to measure the rate constant of the hydroxylation step, which cannot be measured directly by the stopped-flow method. The data also provided independent measurements of rate constants in addition to the values based on flavin absorbance change. The rate constants of the hydroxylation step at various pH values are in the range of 15–17 s^{-1}. These values agree well with the previous approximation (17–21 s^{-1}) based on a lag phase prior to flavin oxidation (39). They are also similar to the hydroxylation rate constant for the reaction of HpaA from *P. aeruginosa* (28 s^{-1}) (40). Unlike HpaA from *P. aeruginosa*, the absorption characteristics of C4a-hydroperoxy-FMN and C4a-hydroxy-FMN bound to C_2 are very similar, preventing the direct measurement of this step by the stopped-flow method. Both C4a-hydroperoxy-FMN and C4a-hydroxy-FMN were nonfluorescent, even when various substrate analogs were used (data not shown). In this respect, C_2 is quite different from many flavin-dependent monooxygenases such as HpaA (40), actinorhodin (44), PHBH (51), phenol hydroxylase (28), and 2-methyl-3-hydroxypyridine-5-carboxylic oxygenase (33, 34) in which the C4a-hydroxy-flavin is more fluorescent than the C4a-hydroperoxy-flavin. Rate constants of the product formation obtained from rapid-quench experiments also indicate that the hydroxylation occurs via a direct participation of the C4a-hydroperoxy-flavin intermediate, as the product formation occurs prior to the flavin oxidation step. In a flavin-dependent halogenase, RebH, product formation takes place long after the flavin reoxidation because the flavin intermediate does not participate directly in the halogenation (43).

Investigation of C_2 reactions in the presence of HPA at various pHs indicated that C_2 efficiently catalyzed hydroxylation reactions throughout a pH range of 6 to 10. Although a quasi-stable C4a-adduct intermediate was less apparent at higher pH, measurements of the hydroxylation rate constants and the total product formation showed that the enzyme did form the intermediate and catalyzed complete oxygenation without generating a significant amount of H_2O_2 from an uncoupling pathway. The decreased amount of C4a-adduct detected at a higher pH value was due to the faster decay of the intermediate (Fig. 7, *step e*). For single-component monooxygenases, an uncoupling pathway, resulting in H_2O_2 generation, is quite common and usually accounts for ~5–30% of the amount of a reducing equivalent (NAD(P)H) consumed (3, 5, 33, 34). It is likely that C_2 achieves this hydroxylation efficiency through optimum interactions among HPA, C4a-hydroperoxy-FMN, and the active site residues. Fig. 1 shows interactions between a hydroxyl group of HPA with two residues in the vicinity, His-120 and Ser-146. The O_4 atom of HPA is 2.8 Å away from the N^{ϵ} of His-120 and 2.82 Å away from the O^{γ} atom of the Ser-146 side chain. This distance allows formation of H-bonding interactions among the -OH group of HPA, N^{ϵ} of His-120, and O^{γ} of Ser-146. These interactions, in turn, can facilitate the electrophilic aromatic substitution mechanism by the convenient removal of the HPA phenolic proton through N^{ϵ} of His-120 (Fig. 9). These residues may also participate in the following process of re-aromatization of the hydroxylated HPA. Besides optimum interactions between the hydroxyl group of HPA and the active site residues, efficient hydroxylation by C_2 implies that the terminal peroxide group of the C4a-hydroperoxy-FMN remains protonated throughout this pH range in order to act as a good electrophile. Although the pK_a of the terminal peroxide group of C4a-hydroperoxide flavin model compounds is approximately 9.2 (63), the active site environment of the flavin-dependent monooxygenase is capable of modulating this pK_a value to act as an electrophile or a nucleophile. Therefore, the pK_a of the C4a-FMN-hydroperoxide in C_2 is likely to be higher than 10, because the hydroxylation efficiency at pH 10 remains as effective as at lower pH. It is possible that His-396, which is in the same vicinity, may facilitate protonation of the terminal hydroperoxide group (Figs. 1 and 9 and Ref. 53).

Only a few single-component, but no two-component, flavin-dependent monooxygenases were investigated for the effects of pH on their reactions. PHBH is a monooxygenase best understood for its monooxygenation mechanism. The rate constant for the hydroxylation increases with higher pH levels, consistent with a pK_a of 7.1 (51). This pK_a value is related to the deprotonation of the substrate (*p*-hydroxybenzoate) phenolic group, which is accomplished through a H-bonding network that is connected to the surface residue, His-72. The H-bonding network in PHBH helps lower the pK_a of the *p*-hydroxybenzoate phenolic group from ~9.3 in the free compound to ~7.1 in the enzyme-bound form (64). The pK_a of the phenolic group of free HPA was measured at 10.4 (data not shown). According to the enzyme-bound HPA structure in Fig. 1, it is possible that the H-atom of the HPA phenolic group forms H-bond interactions with His-120 and Ser-146, which can facilitate proton removal during hydroxylation (Fig. 9). Therefore, factors facilitating the electrophilic aromatic

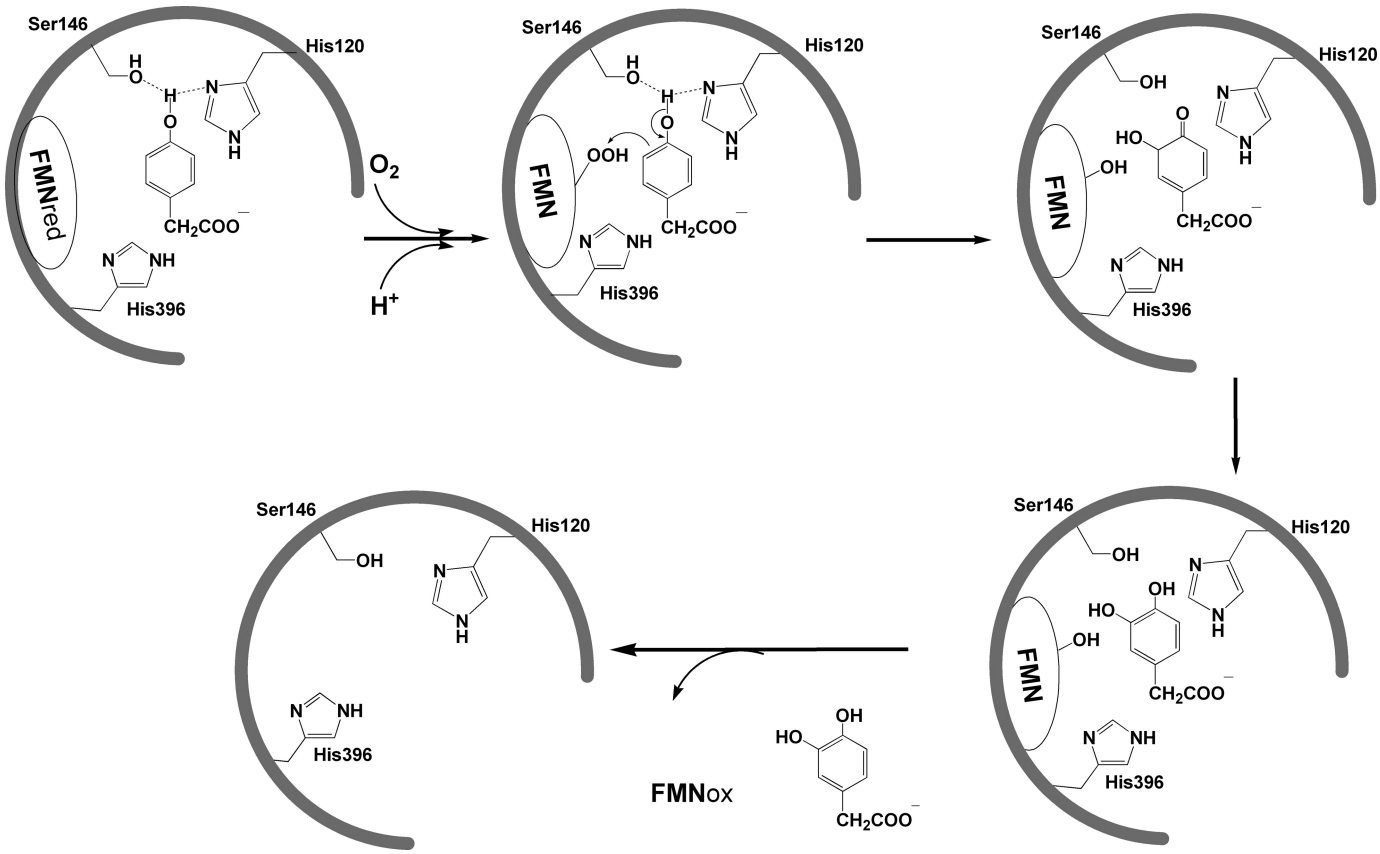

FIGURE 9. **A proposed scheme explaining electrophilic aromatic substitution of HPA in the C_2 reaction.**

substitution in C_2 and PHBH may be different because of the differences in their active site environments. The results from pH-dependent studies of cyclohexanone monooxygenase show that C4a-hydroperoxy-FAD interconverts to C4a-peroxy-FAD with a pK_a of 8.4. For this enzyme, the nucleophilic C4a-peroxy-FAD intermediate is required to attack cyclohexanone to form an oxygenated product (31). Studies of pH dependence in phenylacetone monooxygenase show that the C4a-adduct intermediate, prior to returning to the oxidized species, is more stable at a lower pH (32).

Our results in Fig. 8 also indicate that at pH 9.0, HPA does not inhibit the dehydration of C4a-hydroxy-FMN to form oxidized FMN, which is quite different from the reaction at pH 7.0 (39). This result also explains why the C4a-adduct intermediate was less apparent in the reactions at higher pH levels (Fig. 4). According to the current model explaining the C_2 reaction at different pHs (Fig. 7), after the hydroxylation occurs (*step b*) at high pH, the resulting C4a-hydroxy-FMN rapidly returns to the oxidized species, causing less accumulation of the intermediate (Fig. 7, *right pathway*). At low pHs, excess HPA binds to the C4a-hydroxy-flavin intermediate, which impedes the rate of return to oxidized FMN (Fig. 7, *left pathway*). The pK_a associated with these two partition pathways is ~7.8 (Fig. 7). We propose that this pK_a value may be associated with the deprotonation of a phenolic group of the enzyme-bound DHPA (the pK_a of free DHPA is 9.8 (65)). When the enzyme is bound to the fully protonated DHPA it may be more susceptible to substrate inhibition than when bound to the deprotonated form (Fig. 7). The substrate inhibition at the dehydration step of C4a-hydroxy-flavin is commonly found for aromatic flavoprotein monooxygenases, *i.e.* in PHBH (5), phenol hydroxylase (28), and 2-methyl-3-hydroxypyridine-5-carboxylic oxygenase (33). Interestingly, HpaA from *P. aeruginosa* does not exhibit this substrate inhibition effect (40). Because of slow product release from the HpaA active site, the binding of excess substrate, which is a major cause of substrate inhibition in other monooxygenases, cannot take place in the HpaA reaction (40). For the C_2 reaction, it is not known why HPA inhibition at pH 9.0 is abolished. It may simply be due to a decrease in proton concentration with increasing pH values, thus allowing rapid flavin N5 proton loss, which initiates the water elimination from C4a-hydroxy-FMN before binding of excess HPA.

In conclusion, our findings show that the oxygenase component of HPAH from *A. baumannii* catalyzes oxygenation very efficiently. The hydroxylation reaction was fully coupled without generating a significant amount of wasteful H_2O_2 at pH 6–10, and the hydroxylation rate constant was constant throughout this pH range. These results suggest that the interactions among HPA, C4a-hydroperoxy-flavin, and the active site residues are optimized to facilitate this efficient hydroxylation. It would be interesting to see if similar findings hold for other two-component monooxygenases. This feature is perhaps an advantage in nature for utilizing two proteins, instead of one, to catalyze monooxygenation.

Acknowledgments—We thank Barrie Entsch, University of New England, New South Wales, Australia, for critical reading of the manuscript. We also thank Maneerat Jattulapa for providing the 3,4-dihydroxyphenylacetate dioxygenase used in our experiments and Kittisak Thotsaporn, Somchart Maenpuen, and Pirom Chenprakhon for assistance and useful discussions during manuscript preparation.

REFERENCES

1. van Berkel, W. J., Kamerbeek, N. M., and Fraaije, M. W. (2006) *J. Biotechnol.* **124,** 670–689
2. Ballou, D. P., Entsch, B., and Cole, L. J. (2005) *Biochem. Biophys. Res. Commun.* **338,** 590–598
3. Palfey, B. A., Ballou, D. P., and Massey, V. (1995) in *Active Oxygen: Reactive Oxygen Species in Biochemistry* (Valentine, J. S., Foote, C. S., Greenburg, A., and Lieberman, J. F., eds) pp. 37–83, Chapman-Hall, Scotland, UK
4. Torres Pazmiño, D. E., Winkler, M., Glieder, A., and Fraaije, M. W. (2010) *J. Biotechnol.* **146,** 9–24
5. Entsch, B., Cole, L. J., and Ballou, D. P. (2005) *Arch. Biochem. Biophys.* **433,** 297–311
6. Palfey, B. A., and McDonald, C. A. (2010) *Arch. Biochem. Biophys.* **493,** 26–36
7. Gunsalus-Miguel, A., Meighen, E. A., Nicoli, M. Z., Nealson, K. H., and Hastings, J. W. (1972) *J. Biol. Chem.* **247,** 398–404
8. Ellis, H. R. (2010) *Arch. Biochem. Biophys.* **497,** 1–12
9. Chaiyen, P., Suadee, C., and Wilairat, P. (2001) *Eur. J. Biochem.* **268,** 5550–5561
10. Kirchner, U., Westphal, A. H., Müller, R., and van Berkel, W. J. H. (2003) *J. Biol. Chem.* **278,** 47545–47553
11. Webb, B. N., Ballinger, J. W., Kim, E., Belchik, S. M., Lam, K. S., Youn, B., Nissen, M. S., Xun, L., and Kang, C. (2010) *J. Biol. Chem.* **285,** 2014–2027
12. Xun, L., and Webster, C. M. (2004) *J. Biol. Chem.* **279,** 6696–6700
13. Perry, L. L., and Zylstra, G. J. (2007) *J. Bacteriol.* **189,** 7563–7572
14. Otto, K., Hofstetter, K., Röthlisberger, M., Witholt, B., and Schmid, A. (2004) *J. Bacteriol.* **186,** 5292–5302
15. Tischler, D., Eulberg, D., Lakner, S., Kaschabek, S. R., van Berkel, W. J., and Schlömann, M. (2009) *J. Bacteriol.* **191,** 4996–5009
16. van Hellemond, E. W., Janssen, D. B., and Fraaije, M. W. (2007) *Appl. Environ. Microbiol.* **73,** 5832–5839
17. Eichhorn, E., van der Ploeg, J. R., and Leisinger, T. (1999) *J. Biol. Chem.* **274,** 26639–26646
18. Zhan, X., Carpenter, R. A., and Ellis, H. R. (2008) *Biochemistry* **47,** 2221–2230
19. Witschel, M., Nagel, S., and Egli, T. (1997) *J. Bacteriol.* **179,** 6937–6943
20. Valton, J., Fontecave, M., Douki, T., Kendrew, S. G., and Nivière, V. (2006) *J. Biol. Chem.* **281,** 27–35
21. Koskiniemi, H., Metsä-Ketelä, M., Dobritzsch, D., Kallio, P., Korhonen, H., Mäntsälä, P., Schneider, G., and Niemi, J. (2007) *J. Mol. Biol.* **372,** 633–648
22. Lin, S., van Lanen, S. G., and Shen, B. (2008) *J. Am. Chem. Soc.* **130,** 6616–6623
23. Yeh, E., Garneau, S., and Walsh, C. T. (2005) *Proc. Natl. Acad. Sci. U.S.A.* **102,** 3960–3965
24. Dong, C., Flecks, S., Unversucht, S., Haupt, C., van Pée, K. H., and Naismith, J. H. (2005) *Science* **309,** 2216–2219
25. Balibar, C. J., and Walsh, C. T. (2006) *Biochemistry* **45,** 15444–15457
26. Heemstra, J. R., Jr., and Walsh, C. T. (2008) *J. Am. Chem. Soc.* **130,** 14024–14025
27. Neumann, C. S., Walsh, C. T., and Kay, R. R. (2010) *Proc. Natl. Acad. Sci. U.S.A.* **107,** 5798–5803
28. Maeda-Yorita, K., and Massey, V. (1993) *J. Biol. Chem.* **268,** 4134–4144
29. Schopfer, L. M., and Massey, V. (1980) *J. Biol. Chem.* **255,** 5355–5363
30. Powlowski, J., Ballou, D., and Massey, V. (1989) *J. Biol. Chem.* **264,** 16008–16016
31. Sheng, D., Ballou, D. P., and Massey, V. (2001) *Biochemistry* **40,** 11156–11167
32. Torres Pazmiño, D. E., Baas, B. J., Janssen, D. B., and Fraaije, M. W. (2008) *Biochemistry* **47,** 4082–4093
33. Chaiyen, P., Brissette, P., Ballou, D. P., and Massey, V. (1997) *Biochemistry* **36,** 8060–8070
34. Chaiyen, P., Brissette, P., Ballou, D. P., and Massey, V. (1997) *Biochemistry* **36,** 13856–13864
35. Suske, W. A., van Berkel, W. J., and Kohler, H. P. (1999) *J. Biol. Chem.* **274,** 33355–33365
36. Crozier-Reabe, K. R., Phillips, R. S., and Moran, G. R. (2008) *Biochemistry* **47,** 12420–12433
37. Suadee, C., Nijvipakul, S., Svasti, J., Entsch, B., Ballou, D. P., and Chaiyen, P. (2007) *J. Biochem.* **142,** 539–552
38. Arunachalam, U., Massey, V., and Miller, S. M. (1994) *J. Biol. Chem.* **269,** 150–155
39. Sucharitakul, J., Chaiyen, P., Entsch, B., and Ballou, D. P. (2006) *J. Biol. Chem.* **281,** 17044–17053
40. Chakraborty, S., Ortiz-Maldonado, M., Entsch, B., and Ballou, D. P. (2010) *Biochemistry* **49,** 372–385
41. Gisi, M. R., and Xun, L. (2003) *J. Bacteriol.* **185,** 2786–2792
42. Kantz, A., Chin, F., Nallamothu, N., Nguyen, T., and Gassner, G. T. (2005) *Arch. Biochem. Biophys.* **442,** 102–116
43. Yeh, E., Cole, L. J., Barr, E. W., Bollinger, J. M., Jr., Ballou, D. P., and Walsh, C. T. (2006) *Biochemistry* **45,** 7904–7912
44. Valton, J., Mathevon, C., Fontecave, M., Nivière, V., and Ballou, D. P. (2008) *J. Biol. Chem.* **283,** 10287–10296
45. Bruice, T. C. (1984) *Isr. J. Chem.* **24,** 54–61
46. Venkataram, U. V., and Bruice, T. C. (1984) *J. Chem. Soc. Chem. Commun.* **14,** 899–900
47. Palfey, B. A., and Massey, V. (1998) in *Comprehensive Biological Catalysis* (Sinnott, M., ed) Vol. 3, pp. 83–154, Academic Press, San Diego
48. Ortiz-Maldonado, M., Ballou, D. P., and Massey, V. (1999) *Biochemistry* **38,** 8124–8137
49. Chaiyen, P., Sucharitakul, J., Svasti, J., Entsch, B., Massey, V., and Ballou, D. P. (2004) *Biochemistry* **43,** 3933–3943
50. Chaiyen, P. (2010) *Arch. Biochem. Biophys.* **493,** 62–70
51. Ortiz-Maldonado, M., Entsch, B., and Ballou, D. P. (2004) *Biochemistry* **43,** 15246–15257
52. Thotsaporn, K., Sucharitakul, J., Wongratana, J., Suadee, C., and Chaiyen, P. (2004) *Biochim. Biophys. Acta* **1680,** 60–66
53. Alfieri, A., Fersini, F., Ruangchan, N., Prongjit, M., Chaiyen, P., and Mattevi, A. (2007) *Proc. Natl. Acad. Sci. U.S.A.* **104,** 1177–1182
54. Arunachalam, U., Massey, V., and Vaidyanathan, C. S. (1992) *J. Biol. Chem.* **267,** 25848–25855
55. Galán, B., Díaz, E., Prieto, M. A., and García, J. L. (2000) *J. Bacteriol.* **182,** 627–636
56. Okai, M., Kudo, N., Lee, W. C., Kamo, M., Nagata, K., and Tanokura, M. (2006) *Biochemistry* **45,** 5103–5110
57. Kim, S. H., Hisano, T., Takeda, K., Iwasaki, W., Ebihara, A., and Miki, K. (2007) *J. Biol. Chem.* **282,** 33107–33117
58. Sucharitakul, J., Chaiyen, P., Entsch, B., and Ballou, D. P. (2005) *Biochemistry* **44,** 10434–10442
59. Sucharitakul, J., Phongsak, T., Entsch, B., Svasti, J., Chaiyen, P., and Ballou, D. P. (2007) *Biochemistry* **46,** 8611–8623
60. Macheroux, P., Ghisla, S., Sanner, C., Rüterjans, H., and Müller, F. (2005) *BMC Biochem.* **6,** 26
61. Merényi, G., and Lind, J. (1991) *J. Am. Chem. Soc.* **113,** 3146–3153
62. Evans, M. G., and Uri, N. (1949) *Trans. Faraday Soc.* **45,** 224–230
63. Eberlein, G., and Bruice, T. C. (1983) *J. Am. Chem. Soc.* **105,** 6685–6697
64. Entsch, B., Palfey, B. A., Ballou, D. P., and Massey, V. (1991) *J. Biol. Chem.* **266,** 17341–17349
65. Ishimitsu, T., Fujiwara, Y., and Hirose, S. (1979) *Talanta* **26,** 67–69